BL07LSU
The University-of-Tokyo Outstation Beamline for Materials Science

The soft X-ray undulator beamline BL07LSU was constructed by the Synchrotron Radiation Research Organization [1], The University of Tokyo, at the long-straight section of SPring-8 and has been devoted to joint research with domestic and international researchers since 2009B. In this article, we report the status of the beamline and introduce selected achievements at experimental stations.

1. Undulator beamline

The high-brilliant soft X-ray undulator beamline, SPring-8 BL07LSU, generates the synchrotron radiation beam of (1) hν: 250-2000eV, (2) E/ΔE: > 10,000, (3) spot-size: < 10μm（zone-plate: 70nm）, (4) flux: 10^{12}photons/s, and (5) variable light polarization. Since 2012B, the beamline offers continuous polarization switching at a frequency of 13 Hz for user experiments at the end-stations.

2. Experimental stations

In 2020, there were five different end-stations at the beamline: (1) time-resolved soft X-ray (TR-SX) spectroscopy, (2) ambient-pressure X-ray photoelectron spectroscopy (AP-XPS), (3) 3D nano-ESCA, (4) ultrahigh-resolution soft X-ray emission spectroscopy (HORNET), and (5) free port. All the stations are opened for users. Innovative developments of novel soft X-ray experiments, such as imaging and magneto-optical spectroscopy, were conducted at the free-port station. Here, we introduce two achievements with users [2,4].

2-1. TR-SX station: Time-resolved X-ray photoelectron diffraction using an angle-resolved time-of-flight analyzer

Photoelectron spectroscopy (PES) has been a powerful experimental approach to probe chemical compositions, electronic states, and the atomic structure of a sample. Recently, the method has been combined with the time-resolved technique, and it has succeeded in tracking these quantities in *real time*. At SPring-8 BL07LSU, time-resolved X-ray photoelectron spectroscopy (XPS) measurements have been conducted, and they have succeeded in revealing electronic evolutions during various photovoltaic events. In the present research, we extended our XPS technique to both time and angle resolutions and demonstrated a time-resolved experiment of X-ray photoelectron diffraction (XPD) with the group of K. Hayashi [2].

The time-resolved measurement was made by a pump-probe method with a combination of pulses of synchrotron radiation (SPring-8 BL07LSU) and laser (BL07LASER). Angle-resolved spectra were taken with a two-dimensional (2D) angle-resolved time-of-flight (2DARTOF) analyzer [4]. The photoelectrons detected at a 2D delay-line detector were recorded with their arrival time (t) and position (x,y) that were converted to energy (E) and 2D emission angles (θ_x, θ_y). Figures 1(a) and 1(b) show the Si 2p XPD patterns of the silicene sample from two different atomic sites, α and β, which appear at different binding energies in XPS (Fig. 1(c)). The photon energy of synchrotron radiation was hν = 300 eV. One can find that the experimental XPS pattern is reproduced as a prominent feature in the simulation. By focusing on the pattern of the β site, the variation was detected with various delay times after the optical pump at hν = 1.5 eV. As shown in

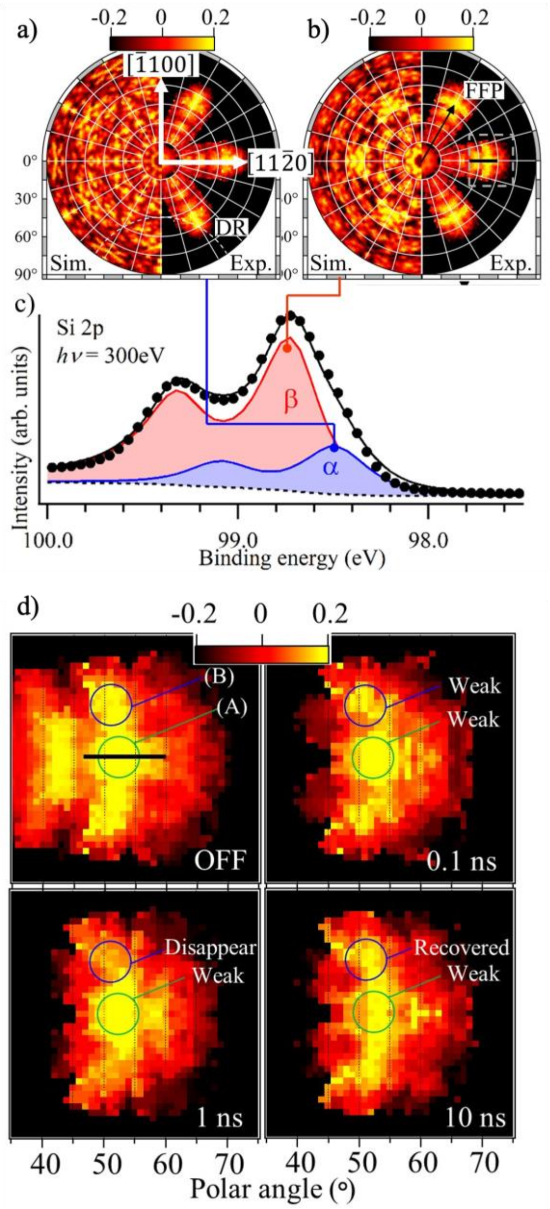

Fig. 1. (a,b) XPD patterns of the Si 2p core levels at the α and β sites in (c) XPS spectrum. (d) Time-resolved XPS pattern of the β site taken at various delay times.

Fig. 1(d), the features, labeled A and B, showed temporal changes, weakening, disappearance, and recovery, during sub-nanoseconds (ns) to 10 ns. These results demonstrate that time-resolved XPD experiments can be effectively made with a 2DARTOF analyzer. The approach can be used to examine the structural changes during dynamical events, such as photo-induced phase transitions.

2-2. HORNET station: Hydrogen-bonded structure of water responsible for ion-selective permeability of self-assembled liquid crystalline polymer membranes

Liquid crystals (LC) are appealing for nanofiltration membranes with uniform sub-nanopores, which enable efficient and thermally stable filtration and ion selectivity. Many principles of water filtration are intuitive: particles bigger than the pore size cannot pass through a membrane, and electrostatic interactions between ions, water molecules, and the membrane can aid the process. However, the permeability of these LC membranes is higher for larger, dianionic SO_4^{2-} ions than for smaller, monoanionic Cl^- ions, which could not be explained using the common filtration principles and implies the presence of another driving force for ion selectivity. One such possibility is the structure of the water surrounding the ions.

Here [3], we investigated the hydrogen-bonded configuration of water molecules in the sub-nanopores of a bicontinuous cubic LC membrane formed by the in situ polymerization of compound 1 (Fig. 2(a)) and how it affects the permeation of dianionic SO_4^{2-} and monoanionic Cl^-. We used high-resolution X-ray emission spectroscopy (XES) to learn how water arranges itself in the sub-nanopores.

XES spectra of pure liquid H_2O absorbed in the LC membrane and hydrating water of the permeating solutes $MgSO_4$ and NaCl were collected at the SPring-8 BL07LSU HORNET station using a high-resolution XES spectrometer [5]. A custom-made ambient pressure cell was used to expose the

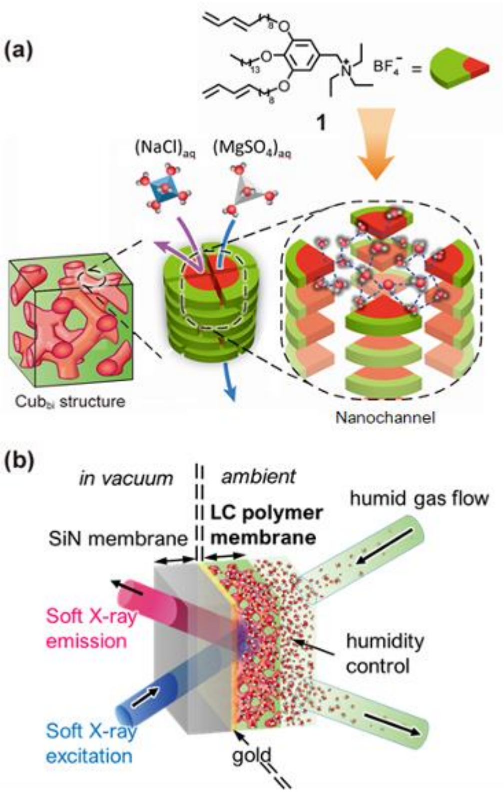

Fig. 2. (a) Molecular structure of an LC monomer (**1**). The monomers were self-assembled to form a bicontinuous cubic (Cub$_{bi}$) LC structure through which ions are selectively transported. (b) Schematic image of soft X-ray emission detection from water in the LC membrane.

LC membrane to humidity-controlled moisture and nitrogen as a carrier gas (Fig. 2(b)). To explore the origin of the selective ion permeation (73±5% for $MgSO_4$ and 30±6% for NaCl), hydrogen-bonded structures of H_2O in the LC membrane were compared with those in the $MgSO_4$ and NaCl hydrations. Spectra of water within the sub-nanopores (Fig. 3(a)) revealed that its hydrogen-bonded network, when confined, loses some structural features of bulk water in favor of new structural features. Very similar structural features are observed in the spectra of the hydration shell of SO_4^{2-} (Fig. 3(b)) but not in those of the hydration shell of Cl^- (Fig. 3(c)). We interpret this as the reason for the membrane permeability of SO_4^{2-} being greater than that of Cl^-. In the near future, computational studies might help understand the exact structure of the hydrogen-bonded network within the sub-nanopores. The nature of hydrogen-bonded networks becomes an additional parameter that should be considered and controlled to obtain highly efficient water filtration.

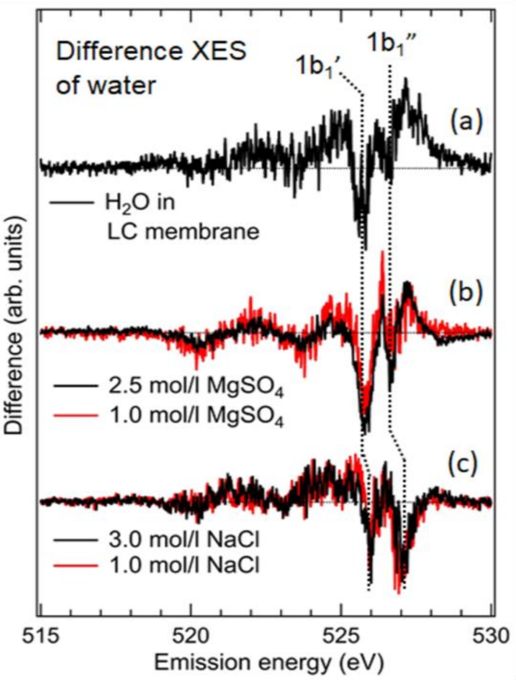

Fig. 3. Valence electronic structure of H_2O in (a) LC membrane, (b) 1.0 and 2.5 mol/l $MgSO_4$, and (c) 1.0 and 3.0 mol/l NaCl aqueous solutions.

Iwao Matsuda, Takashi Kimura, and Yoshihisa Harada

Synchrotron Radiation Research Organization, The University of Tokyo (Institute for Solid State Physics, The University of Tokyo)

References:

[1] http://srro.u-tokyo.ac.jp/

[2] Ang, A. K., Fukatsu, Y. Kimura, K. Yamamoto, Y. Yonezawa, T. Nitta, H. Fleurence, A. Yamamoto, S. Matsuda, I. Yamada-Takamura, Y. & Hayashi, K. (2020). *Jpn. J. Appl. Phys*. **59**, 100902.

[3] Watanabe, R. Sakamoto, T. Yamazoe, K. Miyawaki, J. Kato, T. & Harada, Y. (2020). *Angew. Chem. Int. Ed*. **59**, 23461.

[4] Ogawa, M. et al. (2012). *Rev. Sci. Instrum*. **83**, 023109.

[5] Harada Y. et al. (2012). *Rev. Sci. Instrum*. **83**, 013116.